



**HAL**  
open science

## Split-Cell Method for grain fragmentation

David Cantor Garcia, Nicolas Estrada, Emilien Azéma

► **To cite this version:**

David Cantor Garcia, Nicolas Estrada, Emilien Azéma. Split-Cell Method for grain fragmentation. Computers and Geotechnics, 2015, 9 p. 10.1016/j.compgeo.2015.02.018 . hal-01140252

**HAL Id: hal-01140252**

**<https://hal.science/hal-01140252v1>**

Submitted on 8 Apr 2015

**HAL** is a multi-disciplinary open access archive for the deposit and dissemination of scientific research documents, whether they are published or not. The documents may come from teaching and research institutions in France or abroad, or from public or private research centers.

L'archive ouverte pluridisciplinaire **HAL**, est destinée au dépôt et à la diffusion de documents scientifiques de niveau recherche, publiés ou non, émanant des établissements d'enseignement et de recherche français ou étrangers, des laboratoires publics ou privés.

# Split-cell method for grain fragmentation

David Cantor<sup>a,\*</sup>, Nicolas Estrada<sup>a</sup>, Emilien Azéma<sup>b</sup>

<sup>a</sup>*Departamento de Ingeniería Civil y Ambiental, Universidad de Los Andes, Bogotá, Colombia*  
<sup>b</sup>*LMGC, Université Montpellier 2 - CNRS, Place Eugène Bataillon, 34095 Montpellier cedex 5, France*

---

## Abstract

This article presents a model of grain fragmentation to be implemented in discrete element methods: the Split-Cell Method (SCM). In this method, the particles are of polygonal shape, and they split into polygonal cells once a certain failure criterion, depending on the forces exerted at the contacts, the size and shape of the grain, and the tensile strength of the material, is satisfied. The SCM is an improvement compared to other methods currently available in the literature, given that it does not restrict the shape of the grains or their fragments, mass is conserved throughout the fragmentation events, and it does not introduce artificial length scales in the system. In order to validate the proposed method, an experiment using plaster particles was conducted and its results were compared to those of a numerical simulation of the same system, finding a good match between both the experiment and the simulation.

*Keywords:* simulation, fragmentation, crushing, discrete element methods

---

## 1. Introduction

Grain fragmentation, also known as grain crushing, can have major effects on the mechanical behavior of granular media. For example, it has been shown that grain fragmentation affects the grain size distribution [1, 2, 3], the solid fraction [4, 5], the shear strength [6], and the yielding surface [7] of granular materials. In addition, grain fragmentation is an important mechanism in various industrial processes and controls the response of different structures built on, or with, granular materials [8, 9, 10].

Despite the importance of grain fragmentation, this phenomenon has been studied scarcely using discrete element methods. In fact, only a few models have been proposed. These models can be classified into three main groups.

In the first type of models, the grains that break are replaced by a set of smaller grains once a rupture criterion is satisfied. Usually, both, grains and fragments, are discs (see Fig. 1), and the rupture criterion is a function of the forces exerted at the particle contacts, the particle size, and the tensile strength of the material (e.g., see Refs. [2, 11, 12, 9, 6, 10]). The main advantage of this

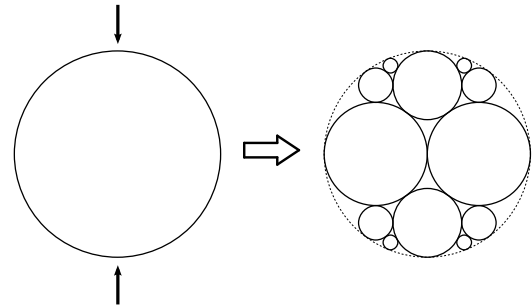


Figure 1: Scheme of the fragmentation process in the first type of models, in which each grain is replaced by a set of smaller grains.

type of models is their simplicity. However, these models introduce unclear features such as the number and size distribution of the fragments, and also some mass is lost as grains break.

In the second type of models, the grains are initially built as clusters of bonded small grains (usually, these small grains are discs or spheres). Then, these bonds are allowed to break during the simulation once a local rupture criterion is satisfied. The de-bonding of the small grains can eventually lead to the rupture of the cluster into fragments (see Fig. 2).

For some examples of works carried out using this technique, see Refs. [13, 14, 15, 16, 17]. The main advantage of this type of models is their ability to re-

---

\*Corresponding author

Email address: da.cantor28@uniandes.edu.co (David Cantor)

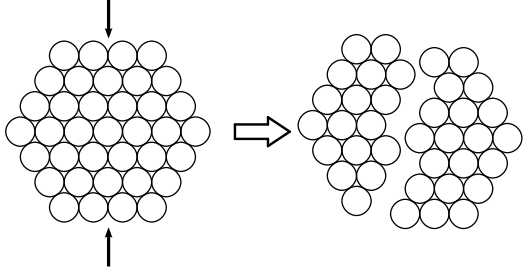


Figure 2: Scheme of the fragmentation process in the second type of models, in which each grain is initially built as a cluster of bonded small grains.

produce, more realistically, the size and shape of the fragments. However, this implies a significant increase of computational cost, given that the “large” grains must be composed of many small bonded grains. Moreover, the size of the small grains introduces an artificial length scale in the system.

In the third type of models, the grains are simulated as deformable objects, by combining a discrete element method with a method derived from continuum mechanics, which allows for the calculation of stresses and strains inside the particle (e.g., see Ref. [18]). These methods are very precise, but this is at the expense of a large computational cost.

The aim of this work was to design, implement, and test a new approach of grain fragmentation: the Split-Cell Method (SCM). This method does not restrict the shape of the grains or their fragments, mass is conserved throughout the fragmentation events, and it does not introduce artificial length scales in the system. The particles are of polygonal shape, and they split into polygonal cells once a certain failure criterion is satisfied. The proposed model can be seen as an extension of the model proposed by Tsoungui [11], since it considers particles of arbitrary shape.

This article is organized as follows. In Sec. 2, the new model is explained in detail. Sec. 3 presents the results of an experiment carried out in order to validate the theoretical model. In Sec. 4, a numerical simulation of the experiment is analyzed, and, finally, in Sec. 5, a summary and a brief discussion are presented.

## 2. Fragmentation model

The fragmentation model is made up of three main ingredients:

- (1) an estimation of the stresses within the grains,
- (2) a failure criterion, and
- (3) a fragmentation mode.

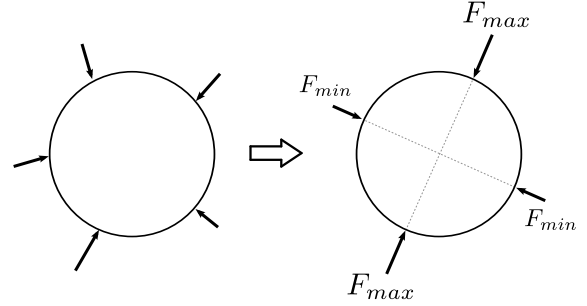


Figure 3: Through the particle stress tensor, it is possible to represent the initial set of forces by a pair of equivalent normal forces applied along the principal directions.

These ingredients are explained in detail in the following subsections.

### 2.1. Stresses estimation

The first step in the model is to estimate the stresses within the grains. Initially, let us consider a circular grain under a certain set of loads. The stress tensor  $\sigma$  of the grain can be calculated as [19]

$$\sigma_{ij} = \frac{1}{V} \sum_{c=1}^{N_c} l_i F_j, \quad (1)$$

where  $V$  is the volume of the grain,  $N_c$  is the number of contacts  $c$ ,  $l$  is the branch vector between the particles in contact, and  $F$  is the contact force. The major principal stress  $\sigma_{\max}$ , the minor principal stress  $\sigma_{\min}$ , and the principal directions are then the eigenvalues and eigenvectors of  $\sigma$ .

Then, it is possible to calculate a pair of equivalent forces that, applied along the principal directions, reproduce the tensor  $\sigma$  (see Fig. 3). These forces, termed here  $F_{\max}$  and  $F_{\min}$ , are given by

$$F_{\max} = \frac{\sigma_{\max} \pi t R}{2}, \quad (2)$$

$$F_{\min} = \frac{\sigma_{\min} \pi t R}{2}, \quad (3)$$

where  $R$  is the radius of the grain, and  $t$  its thickness.

If it is assumed that the grain is made of a brittle material that deforms elastically, it can be shown that each of the equivalent forces,  $F_{\max}$  and  $F_{\min}$ , produces a compression stress along its direction of action and a tensile stress along the orthogonal direction (see Fig. 4). The maximum tensile stress occurs at the center of the grain and is given by

$$\sigma_t^d = \frac{F}{\pi t R}, \quad (4)$$

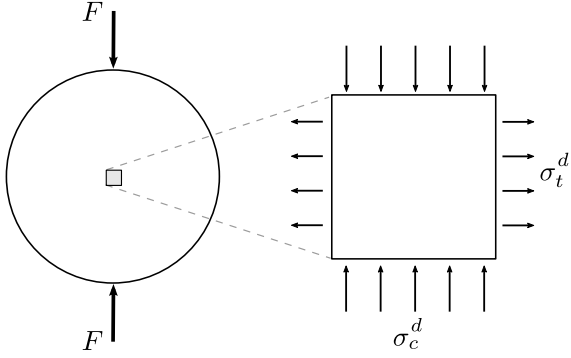


Figure 4: Schematic representation of the stresses at the center of a circular grain loaded diametrically.

where the superscript  $d$  indicates that the calculation only applies for discs, and  $F$  is the diametral load. The compressive stress at the center of the grain is given by

$$\sigma_c^d = \frac{3F}{\pi t R}. \quad (5)$$

The net tensile stress  $\sigma_{t_{\text{net}}}^d$  at the center of the grain can then be calculated as the superposition of the stresses due to forces  $F_{\text{max}}$  and  $F_{\text{min}}$ :

$$\sigma_{t_{\text{net}}}^d = \frac{1}{\pi t R} (F_{\text{max}} - 3F_{\text{min}}). \quad (6)$$

As mentioned in the previous paragraph, Eqs. (4) to (6) are valid only for circular grains. For different grain shapes, a correction must be introduced. Since there is no analytical solution for the stresses within a grain of arbitrary shape, a series of numerical tests were performed using the finite element software ABAQUS, using the linear elastic material behaviour, a Young's modulus of 21 GPa, and a Poisson's ratio of 0.3. In these tests, a set of grains of unit area and different shapes (i.e., regular and irregular polygons with different aspect ratio) were loaded diametrically with a unit vertical load. Figure 5 shows the tensile stress distribution obtained in some of the conducted tests. For each of these tests, the location and direction of the maximal tensile stress was determined, finding that, in most cases, its location was close to the grains center of mass and its direction was orthogonal to that of the unit load. The direction of the maximum compressive stress in the same point was found to be close to that of the unit load.

Figure 6 shows the magnitude of the maximal tensile stress and the orthogonal compressive stress,  $\sigma_t$  and  $\sigma_c$  respectively, in the same location, as functions of the dimensionless shape parameter  $\bar{l}/w$ , where  $\bar{l}$  is the

mean length of the sides intersected by the load direction and  $w$  is the particles' width (see the inset in Fig. 6(a) for a graphical explanation). It can be seen that  $\sigma_t$  decreases with  $\bar{l}/w$ , from  $\sim 0.6$ , which corresponds to a disc (i.e., Eq. (4)), to 0, which corresponds to a square. The stress  $\sigma_c$  also decreases with  $\bar{l}/w$ , from  $\sim 2$ , which corresponds to a disc (i.e., Eq. (5)), to 1, which corresponds to a square.

Then, a simple way to estimate  $\sigma_t$  and  $\sigma_c$  is to consider a linear function joining the data points corresponding to the disc and the square, which leads to

$$\sigma_t = \sigma_t^d \left(1 - \frac{\bar{l}}{w}\right), \quad (7)$$

$$\sigma_c = \sigma_c^d \left(1 - \frac{\bar{l}}{w}\right) + \frac{\bar{l}F}{w^2 t}, \quad (8)$$

where  $\sigma_t^d$  and  $\sigma_c^d$  are given by Eqs. (4) and (5) considering a disc with the same area as the polygon. Note that, in some exceptional cases,  $\bar{l}/w$  can exceed unity. In our model, whenever this happens,  $\bar{l}/w$  is set to unity.

Finally, after superposing both stresses, the net tensile stress for the polygon can be written as

$$\sigma_{t_{\text{net}}} = \frac{F_{\text{max}}}{\pi t R} \left(1 - \frac{\bar{l}_{\text{max}}}{w_{\text{max}}}\right) - \frac{3F_{\text{min}}}{\pi t R} \left(1 - \frac{\bar{l}_{\text{min}}}{w_{\text{min}}}\right) + \frac{\bar{l}_{\text{min}} F_{\text{min}}}{w_{\text{min}}^2 t}, \quad (9)$$

where the subscript "max" refers to the force and dimensions of the grain obtained from the major principal stress value and orientation, and the subscript "min" to those based on the minor principal stress.

The dispersion of the data points in Fig. 6, with respect to the lines drawn from Eqs. (7) and (8), evidences that predicting the stresses inside a particle of arbitrary geometry is a complex problem. Probably, classifying the particles into subgroups of similar geometry and designing a set of equations for each of these subgroups could reduce this dispersion. However, for the sake of simplicity it was decided not to do so, nevertheless achieving, as it will be shown in the following sections, a good match between experiments and simulations.

## 2.2. Failure criterion

The failure criterion determines the stress condition for which a grain must be fragmented. In this model, it is assumed that this occurs when the net tensile stress equals the tensile strength of the material. That is, if

$$\sigma_{t_{\text{net}}} \geq \sigma_{\text{crit}}, \quad (10)$$

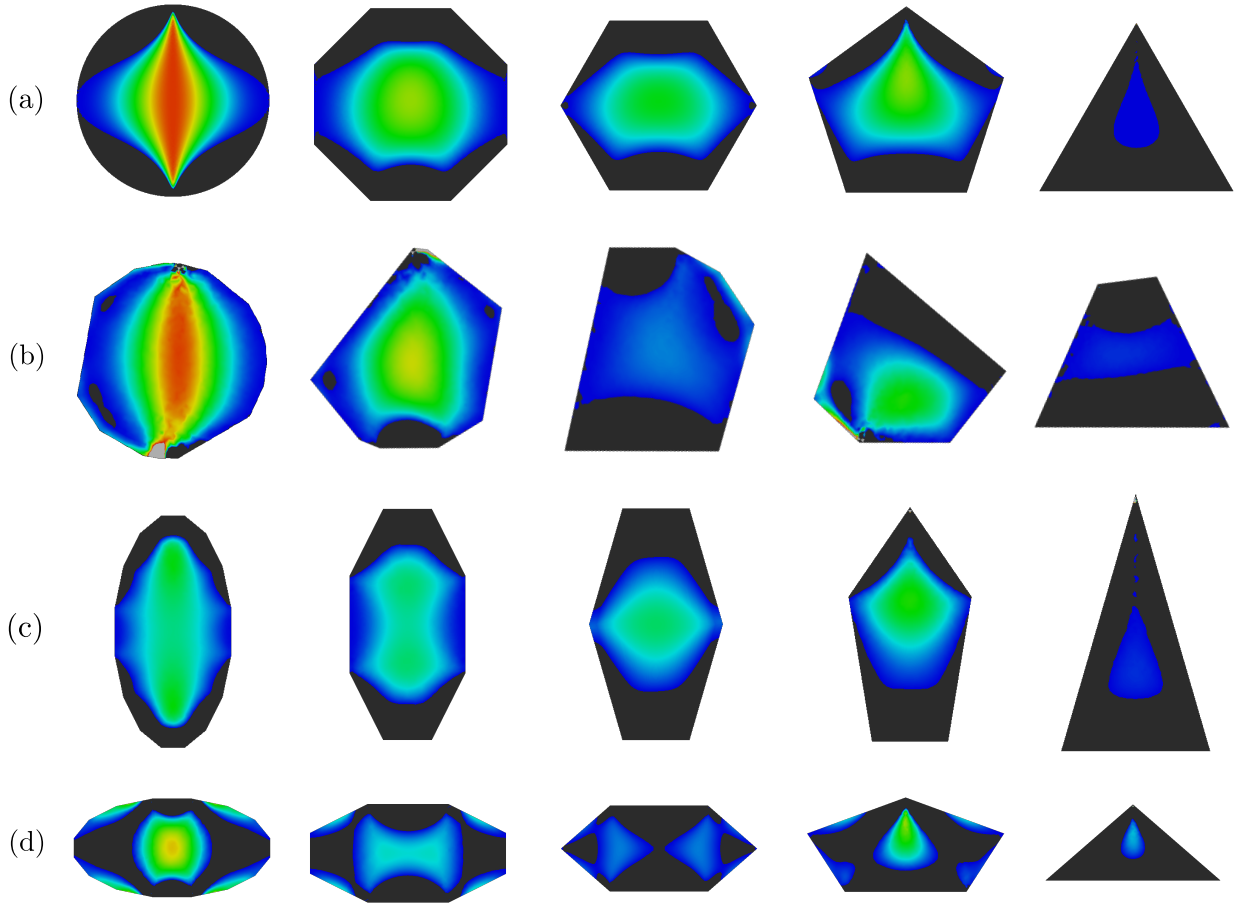


Figure 5: Distribution of tensile stresses in (a) regular, (b) irregular, (c) vertically elongated, and (d) horizontally elongated grains loaded diametrically with a unit vertical load.

then the grain must break. This implies that the model only considers rupture due to tensile stresses, and ignores other modes of failure such as shear or flexion. This is a choice made for the sake of simplicity, supported by field observations on shallow deposits of granular materials on which failure due to tensile stresses is known to be the dominant fragmentation mechanism [20, 21]. Finally, note that the tensile strength is the only parameter this model requires, and this value can be easily found through the indirect tensile test (a.k.a., the Brazilian Test).

### 2.3. Fragmentation mode

The fragmentation mode determines the way in which a grain that satisfies the failure criterion must break. In this Split-Cell Method, this is done by splitting the original grain into two fragments separated by

a line that passes through the grain center of mass and whose orientation is equal to that of the major principal stress (see Fig. 7).

## 3. Experiments

In order to validate the proposed fragmentation model, a set of experiments was conducted. First, a number of diametral load tests were undertaken in order to find the tensile strength of the material. Then, an oedometric compression test in plane strain conditions with several polygonal particles was carried out. The results of both experiments are described in the following subsections.

### 3.1. Tensile strength of the material

The material used in the experiments was plaster powder that, once blended with water, was placed in

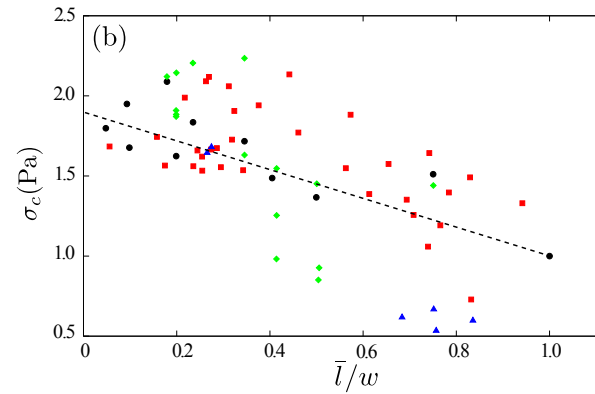
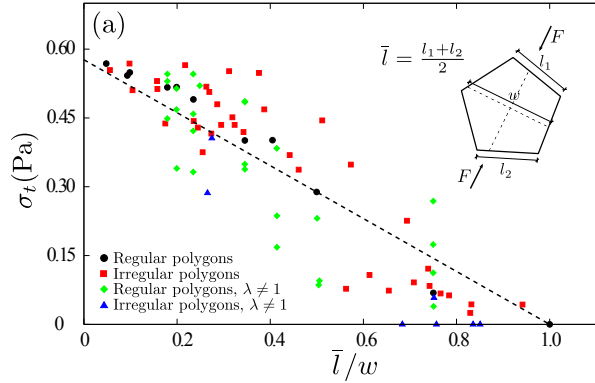


Figure 6: (a) Maximal tensile stress  $\sigma_t$  and (b) orthogonal compressive stress  $\sigma_c$  in the same location, as functions of the dimensionless shape parameter  $\bar{l}/w$  (see the inset for a graphical explanation).

molds and dried out in an oven at 110 °C for 24 hours. A total of twelve circular particles were built and then brought to failure in diametral compression tests. These particles had a thickness of 6 mm and a diameter that varied between 1 and 3 cm. Figure 8 shows a close-up of the loading device, and the corresponding photographs of the particles before and after the diametral compression test. Note that the failure of the particles occurred, on average, along a principal vertical crack (i.e., along the load direction), clearly due to horizontal tensile stresses.

Figure 9 shows the vertical force measured in one of the diametral compression tests as a function of time. It can be seen that the force increases until, eventually, the particle breaks and the force drops abruptly. The maximal force  $F_{crit}$  can be related to the tensile strength of the material as follows

$$\sigma_{crit} = \frac{F_{crit}}{\pi t R}. \quad (11)$$

From the diametral compression tests, performed on the

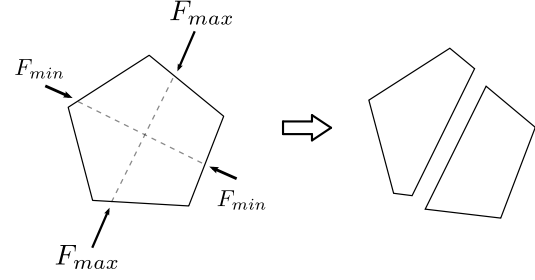


Figure 7: Schematic explanation of the Split-Cell Method.

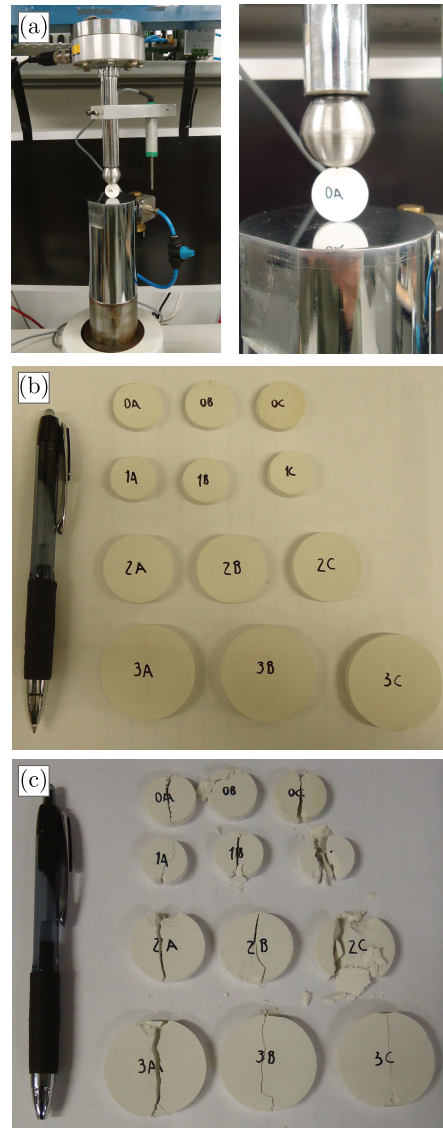


Figure 8: (a) Picture and close-up of the loading device (i.e., diametral compression experiment). Pictures of the discs before (b) and after (c) the experiment.

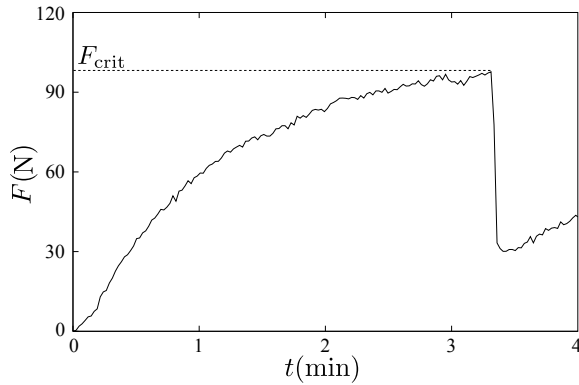


Figure 9: Vertical force as a function of time on a diametral compression experiment.

twelve particles, an average tensile strength of 800 kPa was determined.

### 3.2. Oedometric compression test

Using the material described in the previous subsection, a set of polygonal particles was built. The circumdiameter of the particles varied between 1 and 3 cm, and their thickness was 6 mm. Using these particles, a disordered system with 15 particles was built inside a Plexiglas box. This system was oedometrically compressed in plane strain conditions at a constant velocity of 1 mm/min. Figure 10 shows two pictures of the experiment, at the beginning and at the end of the test. It can be seen that fragmentation occurred in some of the particles while others remained intact.

It is important to mention that a total of four tests were performed; however, only one of them is presented in this paper since similar results were obtained in the other three.

## 4. Simulation and model validation

In order to validate the model, a simulation of the oedometric compression experiment described in the previous section was undertaken. The simulations were carried out using the contact dynamics method [22, 23, 24, 25, 26], which assumes perfectly rigid particles interacting through mutual exclusion and Coulomb friction. For specific implementation of the contact dynamics method, see Ref. [26] and the Appendix in Ref. [27] for polygonal particles<sup>1</sup>. In order to carry out this simulation, it was necessary to measure the friction coefficients between the particles and between the particles

<sup>1</sup>Note that the LMGC90 platform, developed in Montpellier by F. Dubois and M. Jean, was used.

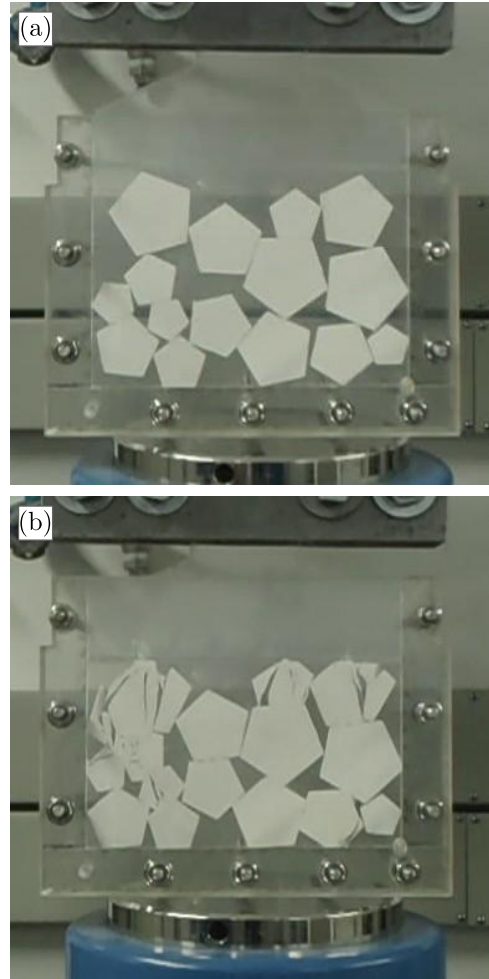


Figure 10: Pictures of the sample at the beginning (a) and at the end (b) of the oedometric compression experiment.

and the Plexiglas walls. These coefficients were measured and set to 0.7 and 0.78, respectively, in the simulation.

Figure 11 shows a comparison between the experiment and the simulation. It can be seen that, even for such a small system (i.e., with only a few particles), the match between the experiment and the simulation is very good in terms of the grains that break, the order of occurrence of the fragmentation events, and even the direction of the cracks.

Quantitatively, one method to measure the damage in the sample, as result of the particles fragmentation, is through the Hardin's parameter ( $B_r$ ) [28]. This parameter defines a damage level as function of the integrals of the granulometric curves before and after a test. Figure 12 shows a scheme of the computation of  $B_r$ .



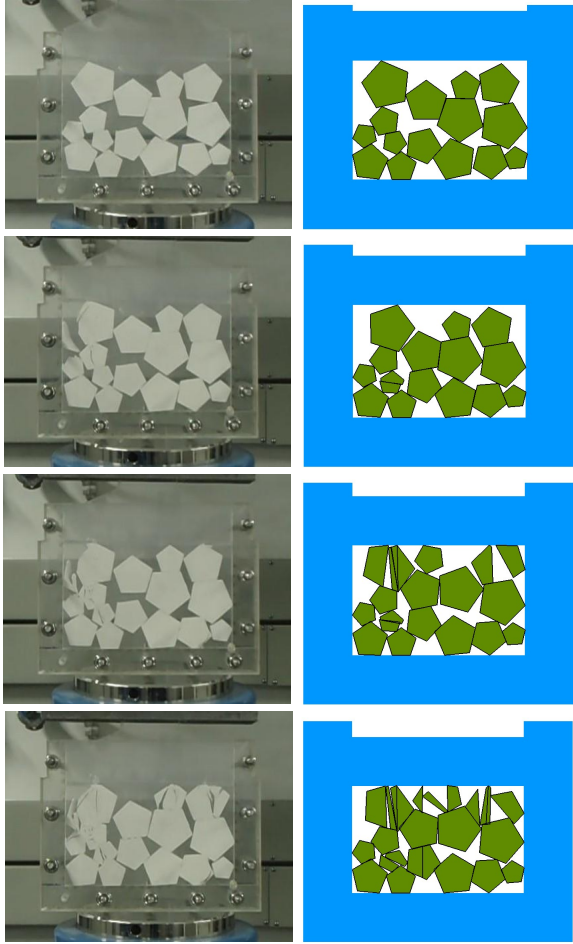


Figure 11: Comparison between the experiment and the simulation.

Figure 13 shows the evolution of the number of fragmentation events, the grain size distribution, and the Hardin's parameter, as functions of the axial strain  $\varepsilon$ , for both the experiment and the simulation.

It should be noted that the comparison started from the first fragmentation event in both systems. Again, it can be seen that the match between the experiment and the simulation is very good, despite the small size of the system.

## 5. Summary and discussion

In sum, this paper presents a new model for implementing the phenomenon of grain fragmentation in discrete element methods: the Split Cell Method (SCM). This model is advantageous, compared to those currently available in the literature, given that it does not restrict the shape of the grains or the fragments, mass is

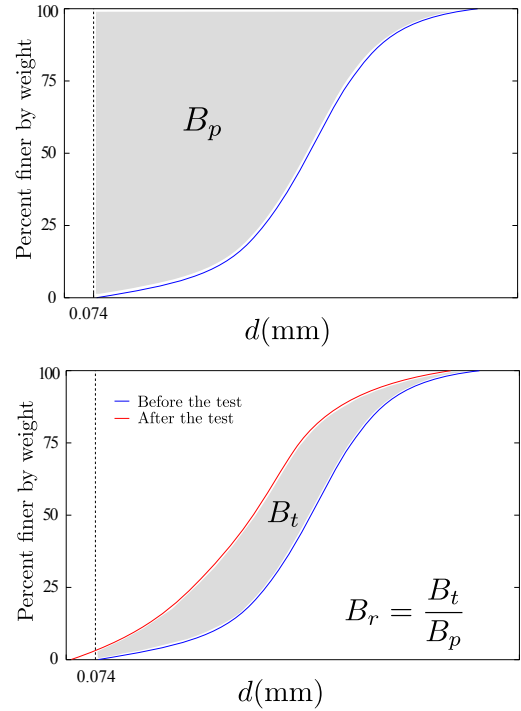


Figure 12: Computation of the Hardin's parameter ( $B_r$ ) as function of integrals (shaded areas  $B_p$  and  $B_t$ ), in the granulometric curves before and after a test. Note that 0.074 mm is the lower bound in the integrals as the fragmentation of smaller soil particles is usually negligible [28].

conserved through the fragmentation events, and it does not introduce artificial length scales in the system. In the SCM, the particles are of polygonal shape, and they split into polygonal fragments once a certain failure criterion is satisfied. This failure criterion is a function of the forces exerted at the contacts, the size and shape of the grain, and the tensile strength of the material. Then, when grains break, they split into two fragments separated by a line that passes through the grain center of mass and whose orientation is equal to that of the major principal stress.

In order to validate the proposed model, an experiment using plaster particles was conducted and its results were compared to those of a numerical simulation of the same system. The system was made up of 15 pentagons of varying size. These particles were placed inside a rectangular box and then compressed in oedometric plane strain conditions.

Firstly, a qualitative comparison was carried out between the experiment and the simulation. It was found that the match was a very good one, in terms of the grains that break, the order of occurrence of the frag-



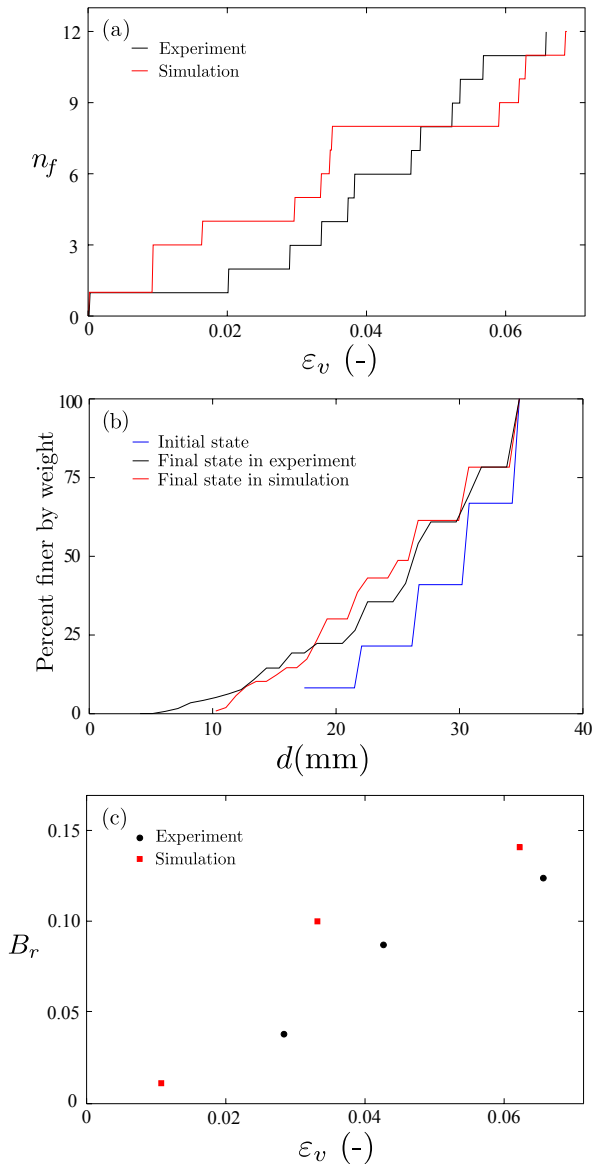


Figure 13: Comparison between the experiment and the simulation of the (a) number of fragmentation events as function of the vertical strain, (b) grain size distribution, and (c) Hardin's parameter as function of the vertical strain.

mentation events, and even the direction of the cracks. Secondly, a quantitative comparison was made in terms of the evolution of the number of fragmentation events, the grain size distribution, and the sample's damage, quantified through the Hardin's parameter  $B_r$ . Again, the match between the experiment and the simulation was very good.

Evidently, grain fragmentation in a real granular ma-

terial is a complex phenomenon that is only partially captured by a model such as the one proposed in this article. In addition, it must be noted that some of the differences identified between the experiment and the simulation were due to the simulation method (i.e., the contact dynamics method), which was chosen because of its advantages for simulating polygonal particles. However, the proposed model is not restricted to this simulation method. In fact, the implementation of the SCM to other formalisms such as the molecular dynamics method with spheropolygons is straightforward and could be an interesting perspective of this work.

We thank in particular Alfredo Taboada and Farhang Radjaï for fruitful discussions. We also acknowledge financial support by the Ecos-Nord program (Grant No. C12PU01).

## References

- [1] G. McDowell, M. Bolton, D. Robertson, The fractal crushing of granular materials, *Journal of the Mechanics and Physics of Solids* 44 (1996) 2079–2101.
- [2] J. Aström, H. Herrmann, Fragmentation of grains in a two-dimensional packing, *The European Physical Journal B* 5 (3) (1998) 551–554.
- [3] T. Fukumoto, Particle breakage characteristics of granular soils, *Soils and Foundations* 32 (1) (1992) 26–40.
- [4] P. Lade, J. Yamamuro, P. Bopp, Significance of particle crushing in granular materials, *Journal of Geotechnical Engineering* 122 (April) (1996) 309–316.
- [5] Y. P. Cheng, Y. Nakata, M. D. Bolton, Micro- and macro-mechanical behaviour of dem crushable materials, *Géotechnique* 58 (6) (2008) 471–480.
- [6] S. Lobo-Guerrero, Visualization of crushing evolution in granular materials under compression using dem, *International Journal of Geomechanics* 6 (June) (2006) 195 – 200.
- [7] N. Miura, H. Murata, N. Yasufuku, Stress-strain characteristics of sand in a particle-crushing region, *Soils and Foundations* 24 (1984) 77–89.
- [8] M. Guimaraes, J. Valdes, A. Palomino, J. Santamarina, Aggregate production: Fines generation during rock crushing, *International Journal of Mineral Processing* 81 (4) (2007) 237–247.
- [9] S. Lobo-Guerrero, L. Vallejo, Dem analysis of crushing around driven piles in granular materials, *Géotechnique* 55 (8) (2005) 617 – 623.
- [10] S. Lobo-Guerrero, L. E. Vallejo, Influence of pile shape and pile interaction on the crushable behavior of granular materials around driven piles: Dem analyses, *Granular Matter* 9 (3–4) (2007) 241 – 250.
- [11] O. Tsoungui, D. Vallet, J. Charnet, Numerical model of crushing of grains inside two-dimensional granular materials, *Powder technology* 105 (1999) 190 – 198.
- [12] V. Buchholtz, J. Freund, T. Pöschel, Molecular dynamics of comminution in ball mills, *The European Physical Journal B* 16 (1) (2000) 169–182.
- [13] R. Jensen, M. Plesha, Dem simulation of particle damage in granular media-structure interfaces, *International Journal of Geomechanics* 1 (1) (2001) 21–39.
- [14] G. McDowell, O. Harireche, Discrete element modelling of soil particle fracture, *Géotechnique* 52 (2) (2002) 131–135.

- [15] W. L. Lim, G. R. McDowell, Discrete element modelling of railway ballast, *Granular Matter* 7 (1) (2005) 19 – 29.
- [16] S. Abe, Grain fracture in 3d numerical simulations of granular shear, *Geophysical Research Letters* 32 (5) (2005) L05305.
- [17] Y. Guo, J. K. Morgan, The frictional and micromechanical effects of grain comminution in fault gouge from distinct element simulations, *Journal of Geophysical Research* 111 (B12) (2006) B12406.
- [18] A. Bagherzadeh-Khalkhali, A. Mirghasemi, S. Mohammadil, Micromechanics of breakage in sharp-edge particles using combined dem and fem, *Particuology* 6 (2008) 347 – 361.
- [19] J. J. Moreau, Numerical investigation of shear zones in granular materials, in: *Friction, Arching, Contact Dynamics*, World Scientific, Singapore, 1997, pp. 233–247.
- [20] J. T. Engelder, Cataclasis and the generation of fault gouge, *Geol. Soc. Am. Bull.* 85 (1974) 1515 – 1522.
- [21] C. G. Sammis, G. King, R. Biegel, The kinematics of gouge deformation, *Pure and Appl. Geophys.* 125 (1987) 777 – 812.
- [22] J. J. Moreau, Some numerical methods in multibody dynamics: Application to granular materials, *European Journal of Mechanics, A/Solids* 13 (Suppl.) (4) (1994) 93 – 114.
- [23] M. Jean, *Mechanics of Geometrical Interfaces*, Elsevier, New York, 1995, pp. 463–486.
- [24] M. Jean, The non smooth contact dynamics method, *Comput. Methods Appl. Mech. Eng* 117 (1999) 235 – 257.
- [25] F. Radjai, V. Richefeu, Contact dynamics as a nonsmooth discrete element method, *Mechanics of Materials* 41 (6) (2009) 715 – 728.
- [26] F. Radjai, F. Dubois, *Discrete-element modeling of granular materials*, ISTE Ltd and John Wiley & Sons, Inc., 2011.
- [27] E. Azéma, N. Estrada, F. Radjai, Nonlinear effects of particle shape angularity in sheared granular media, *Phys. Rev. E* 86 (2012) 347 – 361.
- [28] B. Hardin, Crushing of soil particles, *Journal of Geotechnical Engineering* 3 (1985) 1177–1192.